

value 13.1 K/kbar for dT/dP (see Figure 4) and the values of ΔS_D from Figure 5, the theoretical value of the volume discontinuity at the phase transition is calculated to range from 0.066 cm³/g at $P = 4$ kbar to 0.074 cm³/g at $P = 8$ kbar. As with the entropy discontinuity, the numerical values of the volume discontinuity are in general agreement with experiment, while the slight increasing trend with pressure is not. The experimental values from ref 2 center about 0.069 cm³/g and those of ref 3 cluster about 0.056 cm³/g. In both data sets there is evidence of a slight decreasing trend with increasing pressure. The source of the incorrectly predicted slope is the too large slope of ΔS_D mentioned above.

In summary, the model of the energetic contributions to the free energy of polyethylene presented here can be used to augment the model of the entropic part of the free energy which was presented in ref 6. The result is a complete model of the HPIP. The model correctly predicts the essential features of the orthorhombic-HPIP phase transition.

Most of the earlier theoretical work on the HPIP has been confined to thermodynamic modeling. Bassett and Turner⁹ deduced the schematic form of the free energy-temperature phase diagram from very general considerations. This line of investigation was advanced by Asai,¹⁰ who employed thermodynamic arguments to predict the pressure dependence of the free energy. Additional analysis of this type can be found in ref 1. This type of theoretical approach makes use of thermodynamic data that must be taken from experiment. Consequently it cannot provide a complete theoretical description of the HPIP. A complete theory of the phase transition must employ a statistical mechanical approach. The author is aware of only three calculations predating the present work (including ref 5 and 6). The earliest is a calculation by Hoffman⁸ which is based on consideration of rigid rotation of chains about their axes. Current structural information

makes it clear that this model is not correct. The same is true of calculations by Pechhold et al.¹³ The kink block model of this reference envisions the chain shortening which accompanies the phase transition as being due to large numbers of trans-gauche-trans-gauche kink block sequences. X-ray structural data¹⁴ are inconsistent with such a highly correlated defect (relative to the all trans) structure. Finally, the statistical analysis of Yamamoto¹⁴ is useful for determining the nature and frequency of occurrence of the structural defects. However, the analysis of this reference relies on detailed X-ray measurements and so is not a first-principles calculation. Further, it does not make connection with the thermodynamic data.

The calculation of this paper (and ref 6) is a statistical mechanical calculation which does not rely on any thermodynamic data specific to the HPIP. It successfully predicts the main thermodynamic properties of the orthorhombic-HPIP phase transition. The structural defects which it considers are consistent with the known structural data.

Registry No. Polyethylene (homopolymer), 9002-88-4.

References and Notes

- (1) The most recent review is: Leute, U.; Dollhopf, W. *Colloid Polym. Sci.* **1980**, *258*, 353.
- (2) Dollhopf, W. Ph.D. Thesis, Ulm, 1979.
- (3) Kotov, N.; Zubov, Y.; Bakeyev, N. *Dokl. Akad. Nauk SSSR* **1976**, *229*, 1375.
- (4) Wunderlich, B.; Grebowicz, J. *Adv. Polym. Sci.*, in press.
- (5) Priest, R. *J. Appl. Phys.* **1981**, *52*, 5930.
- (6) Priest, R. *Macromolecules* **1982**, *15*, 1357.
- (7) Pastine, D. J. *J. Chem. Phys.* **1968**, *49*, 3012.
- (8) Hoffman, J. D. *J. Chem. Phys.* **1952**, *20*, 541.
- (9) Bassett, D. C.; Turner, B. *Philos. Mag.* **1974**, *29*, 925.
- (10) Asai, K. *Polymer* **1982**, *23*, 391.
- (11) Scott, R. A.; Scheraga, H. A. *J. Chem. Phys.* **1967**, *44*, 3054.
- (12) The numerical values for α_{\max} are used for $R < 0.38$.
- (13) Pechhold, W.; Liska, E.; Grossmann, H. P.; Hagele, P. C. *Pure Appl. Chem.* **1976**, *46*, 487.
- (14) Yamamoto, T. *J. Macromol. Sci., Phys.* **1979**, *B16*, 487.

Notes

Monte Carlo Simulation of Polymerization with Reversible Chain Transfer

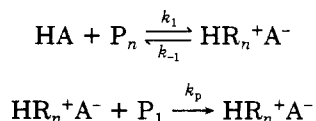
KENNETH F. O'DRISCOLL

Department of Chemical Engineering, University of Waterloo, Waterloo, Ontario N2L 3G1, Canada.
Received November 28, 1984

In a recent paper,¹ Szwarc and Zimm have shown that the model which represents the experimental work of Kennedy et al.² (Scheme I) can be represented by a set of differential equations which they solved numerically.

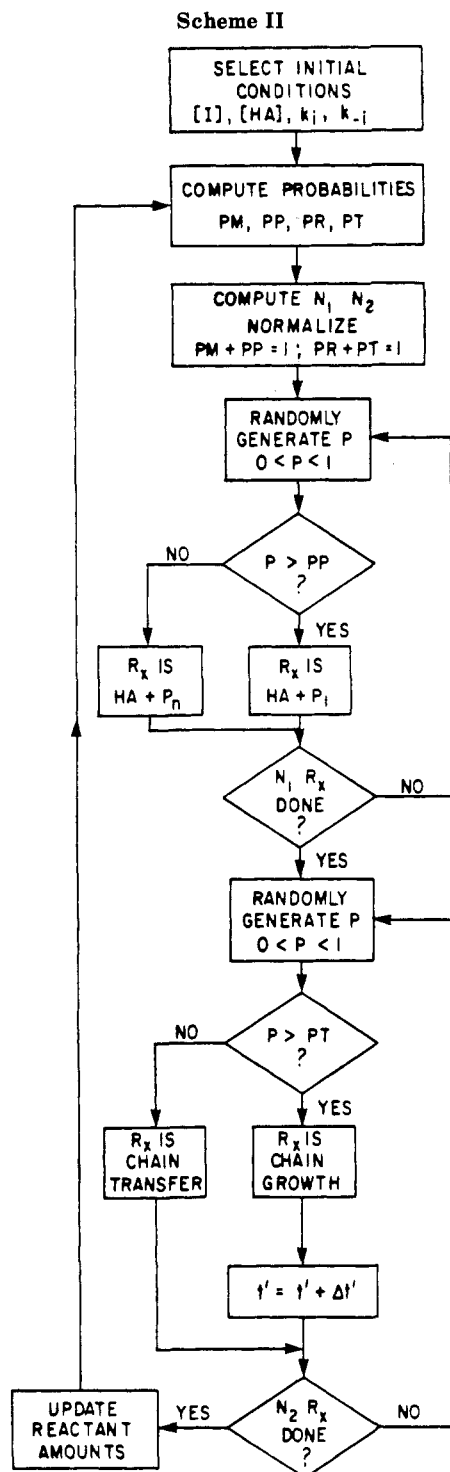
In Scheme I, initiator HA reacts reversibly with monomer, P_1 , or dead polymer, P_n , to form live polymer $HR_n^+A^-$; the latter species propagates by irreversible addition of monomer; its loss of HA when $n > 1$ is in effect a spontaneous chain transfer.

Scheme I



Some difficulty was experienced in the numerical solution of the model on a VAX 11-780 because of the equations' stiffness;¹ further tests of the authors' conclusions were restricted by the magnitude of the variables needed in the numerical differential equation solution. Even so they were able to establish conclusively some rather interesting points about the kinetics of Scheme I. One of these concerned the polydispersity of the molecular weight distribution $R = \bar{P}_w/\bar{P}_n$, which was expected to approach $4/3$ at long times; the value of $4/3$ was arrived at by deduction from an analytical solution possible for long times. However, the computer solution indicated the polydispersity approaching what might be a maximum at $R = 1.5$; long-time solutions, where R might approach $4/3$, were not possible with the resources available. An unexpected (and unexplained) behavior of the R vs. time plot was a hump at short times, which was seen in more than one calculation.

There are essentially two ways to solve the kinetics of a polymerization model: one is to solve differential equations, analytically or numerically, and the other is to use Monte Carlo simulations. Either method requires the same input information and is capable of producing the



same output information. The choice of one method over the other is really only a question of taste or convenience, except when analytical solution is impossible or computer time is limited. In some instances, the Monte Carlo method may be less demanding of computer time or more attractive because it permits better conceptual understanding of the kinetic process.

Simulation

With the above thinking in mind, I simulated Scheme I by a Monte Carlo routine on an Apple II computer. (For a general discussion of Monte Carlo simulations, see ref 3.) The algorithm used is shown in Scheme II. Absolute probabilities of reaction were computed for the initiator HA reacting with monomer (PM) or dead polymer (PP)

and of live polymer propagating (PR) or undergoing chain transfer (PT).

$$PM = k_1[HA][P_1] \quad (1)$$

$$PP = k_1[HA][P_n] \quad (2)$$

$$PR = k_p[HR_n^+A^-][P_1] \quad (3)$$

$$PT = k_{-1}[HR_n^+A^-] \quad (4)$$

Square brackets here denote the number of molecules being considered in the Monte Carlo simulation.

Relative values of rate constants and initiator concentrations used in this work were the same as those chosen for examination by Szwarc and Zimm:¹ $k_p = 1$, $k_1 = 0.2$, $k_{-1} = 0.02$, and $[HA]_0 = [P_1]$; the monomer concentration was kept constant throughout the simulation, with $[P_1] = 1000$.

A number of events (N) equal to the sum of all four reactions was arbitrarily set, typically at 400. Some number (N_1) of these events were the reactions of HA; another number (N_2) of them were reactions of the live chains. Events from the set N_1 were deemed to be proceeding concurrently with events from the set N_2 . The numbers of those events were computed from the relative probabilities

$$N_1 = N(PM + PP)/(PM + PP + PR + PT) \quad (5a)$$

$$N_2 = N(PR + PT)/(PM + PP + PR + PT) \quad (5b)$$

After doing N_1 events of adding monomer or dead polymer to HA according to the usual Monte Carlo manner, using computed probabilities, and storing the results, the program similarly performs $N_2 = N - N_1$ events which propagate the chain or cause chain transfer. These results are also stored. Then the program loops to recalculate probabilities (a necessity because concentrations have been changed during the execution of N events) and does N events once again. This continues, with storage of results, until a desired time of reaction is reached or memory of the computer exhausted.

The only unusual feature of this algorithm is the necessity to include an internal "clock" so that the time of reaction can be recorded. This was done using the Szwarc-Zimm parameter

$$t' = k_p[P_1]t \quad (6)$$

so that the Monte Carlo results might be directly compared with the numerical solution of the differential equations.

One incremental unit of time, Δt , in the simulation is the time required to add one monomer and is given by the reciprocal of the rate of propagation for the set of monomers being considered in the Monte Carlo simulation:

$$\Delta t = 1/PR \quad (7)$$

In dimensionless time this is

$$\Delta t' = \Delta t(k_p[P_1]) = 1/[HR_n^+A^-] \quad (8)$$

Therefore, every simulation even which resulted in the addition of a monomer to a chain was equivalent to increasing t' by one unit of numerical value $\Delta t'$.

Discussion of Results

The simulation was done with those values of rate constants explored by Szwarc and Zimm.¹ Although attainment of equilibrium between growing and dormant polymers could not be achieved (as was possible in the differential equation work¹), Figure 1 shows that the same polydispersity change with time could be observed. Unfortunately, the Apple memory was too small to extend to

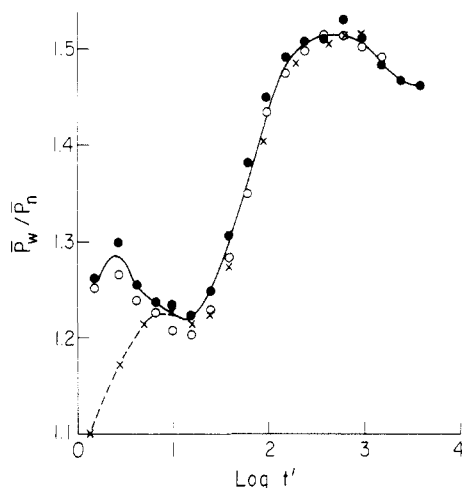


Figure 1. \bar{P}_w/\bar{P}_n as a function of dimensionless time simulated by Monte Carlo on the Apple (○) and IBM (●) and by numerical solution of differential equations¹ (×).

longer times, so the same simulation was done on an IBM 4341, with the result also shown in Figure 1. It can be seen that the hump at low time was observed for all three sim-

ulations; it is most likely that the difference in time when the hump is observed in the Monte Carlo simulation compared to that in the numerical equation simulation is attributable to the difficulty in establishing equilibrium concentrations of the various propagating species. Nevertheless, the present observation of the hump sustains the contention¹ that it is not an artifact of the numerical differential equation solution; further, Figure 1 shows that the possible maximum in R observed by Szwarc and Zimm is truly a maximum but that the expected decline to $R = 4/3$ (which they could not observe) occurs on a time scale so slow as to be unapproachable in real systems.

Acknowledgment. Support of this work by the Natural Sciences and Engineering Research Council of Canada is appreciated, as is the adapting of the Apple program to the IBM by T. Duever.

References and Notes

- (1) M. Szwarc and B. H. Zimm, *Macromolecules*, **16**, 1918 (1984).
- (2) J. P. Kennedy and T. Kelen, *J. Macromol. Sci., Chem.*, **A18**, 1189 (1983).
- (3) G. G. Lowry, "Markov Chains and Monte Carlo Calculations in Polymer Science", Marcel Dekker, New York, 1970.

Communications to the Editor

A Novel Fluorescence Technique for Monitoring Cure Reactions in Epoxy Networks

Properties of network polymers depend on the characteristics of network structure, namely, the number of cross-links and branch points. In order to correlate the structure with the properties of network polymers, it is therefore necessary to quantify such structural characteristics. To achieve this, we recently reported on a new technique for characterizing cure of epoxy by the azochromophore labeling method.^{1a} In that technique, we use a small amount of *p,p'*-diaminoazobenzene (DAA) as a reactive label in a model epoxy consisting of the diglycidyl ether of bisphenol A and diaminodiphenyl sulfone (DGEBA-DDS). The reactivities of DDS and DAA are similar,² allowing us to follow the cure process as manifested by the UV-vis spectral changes of DAA occurring above 400 nm. As the epoxy is cured, the λ_{max} of the $\pi \rightarrow \pi^*$ transition corresponding to the azo bond of DAA shows red shifts allowing the spectral discrimination for four major cure products, namely, cross-links, branch points, linear chains, and chain ends. Deconvolution of the UV-vis spectra based on the band assignments of the model compounds^{1b} representing cure products provides a quantitative estimate of the four cure products as a function of temperature or cure time. Our analyses showed the number of the branch points and the cross-links increasing near gelation, followed by leveling off after vitrification.¹ Such a leveling off is expected due to the difficulty in diffusion (or mobility) of the reactants (or reactive functional groups) after vitrification and supported by IR spectroscopy on epoxy ring disappearance.¹

We recently found that DAA-labeled epoxy (DGEBA-DDS) exhibits very sensitive changes in fluorescence intensity corresponding to the emission by the DAA label as a function of cure extent. This change in fluorescence

behavior is not due to the viscosity or mobility changes as the polymerization proceeds, as exploited by many researchers.³ Rather, it is attributed to the formation of DAA-labeled cure products which exhibit much greater fluorescence intensity as compared to DAA itself. This increase in fluorescence intensity is due to the overlap of the red-shifted $\pi \rightarrow \pi^*$ transition and the unshifted $n \rightarrow \pi^*$ transition in N-alkylated aminoazobenzene.⁴ Pan and Morawetz used a fluorescing reagent which is converted to a nonfluorescent product for the kinetic analyses of acylation of aromatic amine residues attached to cross-linked polymers.⁵ In this communication, we present data that demonstrate this novel fluorescence technique for monitoring cure reactions in an epoxy network.

The epoxy under study is the same as reported in ref 1, i.e., a stoichiometric mixture of DGEBA-DDS epoxy containing a small amount of DAA (0.1–0.3% by weight). Both DGEBA and DDS show strong fluorescence around 380 nm when excited at their absorption maxima, 330–340 nm. However, the fluorescence beyond 400 nm is negligible. The fluorescence intensity at 380 nm is independent of cure extent, which is consistent with the findings of Levy and Ames.⁶

When this DAA-containing epoxy is excited at 456 nm or near the red-shifted λ_{max} of the UV-vis spectra as cure proceeds, we observed sharply increasing fluorescence centered around 560 nm. Figure 1 illustrates such an s-shaped fluorescence intensity curve as a function of cure time at 160 °C. When the upper part of the curve is extrapolated, its intersection with a tangent to the inflection point of the curve defines a transition time t^* . At 160 °C, it turned out to be 50 min. Similar s-shaped curves were obtained at 180 °C as well as 140 °C, with t^* being 20 and 80 min, respectively (Figure 2). These time scales are very close to the gel time as reported by the T-T-T diagram of this epoxy.⁷